

Efficient Extreme UV Harmonics Generated from Picosecond Laser Pulse Interactions with Solid Targets

P. A. Norreys,¹ M. Zepf,² S. Moustazis,³ A. P. Fews,⁴ J. Zhang,² P. Lee,⁵ M. Bakarezos,³ C. N. Danson,¹ A. Dyson,⁵ P. Gibbon,⁶ P. Loukakos,³ D. Neely,¹ F. N. Walsh,¹ J. S. Wark,² and A. E. Dangor⁵

¹Rutherford Appleton Laboratory, Chilton, Didcot, Oxon, OX11 0QX, United Kingdom

²Department of Physics, Clarendon Laboratory, University of Oxford, Parks Road, Oxford, OX1 3PU, United Kingdom

³IESL/FORTH, University of Crete, P.O. Box 1527, 711 10 Heraklion, Crete, Greece

⁴H. H. Wills Physics Laboratory, University of Bristol, Tyndall Avenue, Bristol BS8 1TL, United Kingdom

⁵Imperial College of Science, Technology and Medicine, Prince Consort Road, London SW7 2AZ, United Kingdom

⁶Max Planck Gesellschaft, Research Unit "X-Ray Optics," University of Jena, Max-Wien-Platz 1, D-07743 Jena, Germany

(Received 24 August 1995)

The generation of high harmonics created during the interaction of a 2.5 ps, 1053 nm laser pulse with a solid target has been recorded for intensities up to 10^{19} W cm⁻². Harmonic orders up to the 68th at 15.5 nm in first order have been observed with indications up to the 75th at 14.0 nm in second-order diffraction. No differences in harmonic emission between *s* and *p* polarization of the laser beam were observed. The power of the 38th high harmonic at 27.7 nm is estimated to be 24 MW.

PACS numbers: 42.65.Ky, 52.40.Nk, 52.50.Jm

There is currently great interest in the production of coherent extreme UV (XUV) radiation by the process of high harmonic generation using high-power picosecond laser radiation. Several groups have had considerable success in generating high odd-order harmonics from gases [1–12], with harmonic orders up to the 141st of Nd:glass (1053 nm) [10], 109th of Ti:sapphire (800 nm) [11], and 37th of KrF (248 nm) at 67 Å (the shortest wavelength to date) being observed [12]. The high harmonics are produced due to the extreme nonlinearity of the atomic polarizability in the intense laser field, with the symmetric nature of the atomic potential dictating that only odd-order harmonics are observed.

In addition to harmonic generation from gaseous targets, there has recently been a renewal in interest in generating high order harmonic radiation from high-power laser interactions with solids [13–17]. Such high harmonics were first observed in nanosecond experiments using CO₂ lasers (where up to the 46th was observed), where the long laser wavelength (10.6 μm) ensured significant ponderomotive steepening of the plasma density profile [18–22]. Both odd- and even-order harmonics are generated via the relativistic current associated with the electrons being dragged back and forth across this asymmetric density step. Recently Gibbon has performed particle-in-cell (PIC) code simulations of laser-solid harmonic generation for subpicosecond pulses [23]. He concludes that for $I\lambda^2 > 10^{19}$ W μm² cm⁻², and modest shelf densities of $N_e/N_{\text{critical}} = 10$, up to 60 harmonics can be generated with power conversion efficiencies of 10^{-6} . Importantly, Gibbon's simulations predict that the harmonic order is simply determined by $I\lambda^2$, thus short wavelength lasers should produce shorter absolute wavelengths for a given value of $I\lambda^2$. Also, short wavelength, intense lasers may eventually provide a route to shorter wavelength, higher

conversion efficiency harmonics than have hitherto been generated.

Recently, the observation of the 15th harmonic was reported from a 130 fs laser-solid interaction using a Ti:sapphire laser at 800 nm with intensities up to 10^{17} W cm⁻² [17]. However, to date, the extremely high orders that have been previously associated with laser-gas interactions and the nanosecond, long wavelength CO₂ laser-solid work have yet to be reproduced with shorter wavelength picosecond lasers incident on solids. An investigation of harmonic generation from solids with picosecond ultrahigh intensity laser pulses is therefore timely.

The work we present in this Letter constitutes the first conclusive evidence of extremely high-order harmonic radiation being produced from a 1053 nm, picosecond laser pulse interacting with a solid. Harmonic orders up to the 68th in first order diffraction with indications of the 75th in second order have been observed with laser intensities on target up to 10^{19} W cm⁻², and with energy conversion efficiencies estimated at ranging from 10^{-4} to 10^{-6} .

The experiment was performed using the chirped pulse amplification beam line on the VULCAN laser at the Central Laser Facility of the Rutherford Appleton Laboratory [24]. The laser produced pulses of 2.5 ps duration and energies of about 20 J on target. The contrast ratio was measured to be better than 10^{-6} using a third order autocorrelator. A single shot autocorrelator allowed individual pulse lengths to be measured. The laser beam was focused onto the target by an *f*/4.2, 44 cm focal length off-axis parabolic mirror.

The laser was incident on the target surface at an angle of 54° to the target normal, and the reflected beam was directed into a modified flat field XUV spectrometer.

X-ray and ion penumbral imaging cameras provided high resolution ($2\ \mu\text{m}$) images of the plasma via a proven maximum entropy deconvolution technique [25]. In addition, CR-39 plastic nuclear track detectors provided ion spectra and maximum ion energies associated with the plasma expansion [26]. These diagnostics allowed the intensity on target to be determined accurately for each shot.

The majority of targets consisted of a $2\ \mu\text{m}$ CH plastic layer coated on 200 nm thick $15\ \mu\text{m}$ wide Al cross wires on 1.5 mm optically polished glass slabs. In some cases a $2\ \mu\text{m}$ CH layer was coated onto metal "sandwich" targets. Targets with a CH overcoat were proven to be the most suitable targets in the experiment due to their lower free-free and free-bound contributions to the spectra.

The harmonic emission was detected with a slitless flat-field grazing incidence XUV spectrometer (1200 line/mm Hitachi grating at 4°) used with an additional gold-coated grazing incidence cylindrical mirror. The grating and mirror were oriented so that their grazing incidence reflections gave perpendicular astigmatic line images of the focus of the laser beam at the detector plane. Their combined effect therefore produced a series of dispersed monochromatic images of the focus at each harmonic wavelength as shown in Fig. 1. The total wavelength coverage was from 15 to 90 nm [27]. The imaging mirror, flat-field grating, and microchannel plate detector plane were located 22.5, 61.5, and 85 cm from the target, respectively. The imaging mirror was set up with a glancing angle of 4° so that the spectrometer intercepted a total solid angle of 3.2×10^{-5} sr. The microchannel plate and charged coupled device (CCD) detector was calibrated against x-ray film and a phosphor and CCD detector [28]. The instrument calibration is accurate to approximately a factor of 6, taking into account the

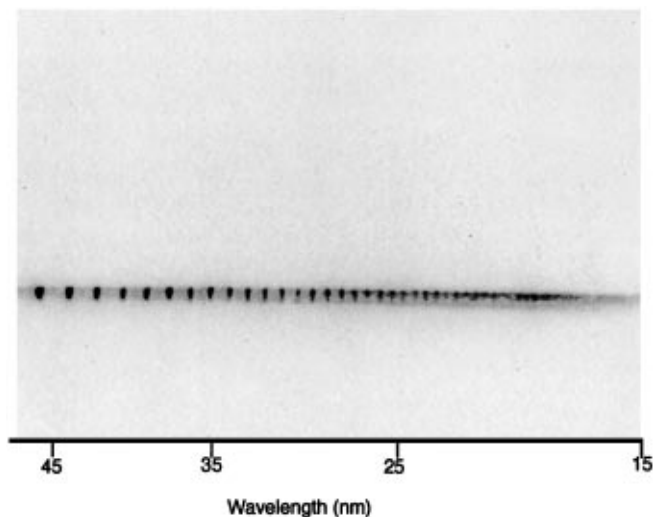


FIG. 1. Harmonic spectrum for an incident irradiance of $I\lambda^2 = 1.0 \times 10^{19}\ \text{W}\ \mu\text{m}^2\ \text{cm}^{-2}$.

uncertainty of the calibration and the reflectivities of the diffraction grating and the grazing incidence mirror.

Figure 1 shows a spectrum taken when 20.7 J of p -polarized laser energy in 2.6 ps was incident on a target consisting of $2\ \mu\text{m}$ CH coating onto a metal sandwich target ($25\ \mu\text{m}$ Mo on $50\ \mu\text{m}$ Pd). The maximum entropy deconvolved x-ray penumbral images established that the spot diameter was $\sim 9\ \mu\text{m}$ full width at half maximum (FWHM), yielding an intensity on target of $9 \times 10^{18}\ \text{W}\ \text{cm}^{-2}$. Figure 2 shows a lineout of the spectrum shown in Fig. 1 in the range 36–15 nm, where the instrument response function has been deconvolved, again using the maximum entropy technique. Harmonic emission up to the 68th order (15.5 nm) can clearly be seen in the first-order diffracted signal, with evidence of up to the 75th order (14.0 nm) visible in the second-order diffraction.

The target was rotated so that the angular distribution of the harmonic emission could be observed (ideally the target position should have remained constant and the spectrometer rotated, but this was impracticable as there were only two positions available on the target chamber). The harmonic emission was observed to have a significantly larger angular distribution than the cone angle of the laser beam. Harmonics were observed when the laser had an angle of incidence between 21.5° and 63° to the target normal (this corresponds to the observation of harmonics over a cone angle varying from -9° to $+22.5^\circ$ with respect to the center of the reflected infrared beam). This observation was confirmed when the angular distribution of the third harmonic emission was measured on a single shot basis by placing a piece of ILFORD HP5 optical film behind an interference filter at a distance of 2 cm from the front of the target. No change in intensity of the third harmonic was observed over an angle of 103° . It is therefore not unreasonable to assume isotropic emission of the

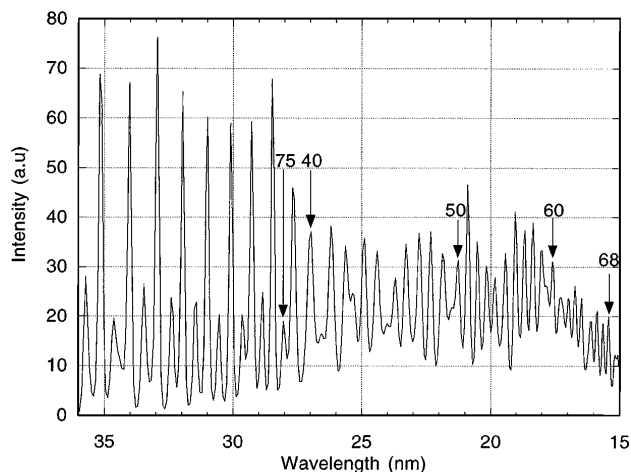


FIG. 2. Lineout from the spectrum in Fig. 1 in the range 36–15 nm after the instrument response function has been removed by a maximum entropy deconvolution procedure.

harmonics which is in keeping with previous high irradiance, nanosecond CO₂ experiments [20].

A prepulse at 10^{-3} intensity level and 2.5 ps duration was introduced into the laser chain 400 ps before the arrival of the main pulse. Again, no difference in harmonic emission was observed with the insertion of this prepulse.

The laser beam was changed from p to s polarization by the insertion of a mica half wave plate after the large area diffraction gratings. No differences in the intensities of the harmonics were observed between the two polarizations of the laser beam.

These effects—no observable difference in harmonic generation between s and p polarizations, the very large angular distribution, and the relative insensitivity to prepulse levels—suggest that the critical density surface is rippled during the interaction, as this blurs the distinction between s and p polarization and accounts for the discrepancies between our observations and theoretical modeling [14,23,29]. For instance, Gibbon predicts a 1/10 reduction in energy conversion for s polarization at 45° incidence angle. Furthermore, these results are consistent with the observations made in the high irradiance CO₂ experiments, where the laser-plasma interaction was made solely with s polarized light [20]. The development of a Rayleigh-Taylor-like instability at the critical surface has been observed in 2.5 dimensional PIC simulations [29,30] when a high intensity, picosecond laser pulse interacts with a preformed plasma. Even with an intensity contrast of 10^{-6} between the 80 ps FWHM duration pedestal (which is the stretched pulse duration in the laser chain) and the 2.5 ps FWHM main pulse, the pedestal level is sufficiently intense to generate a preformed plasma at these focused intensities. However, these simulations also predict that the ponderomotive pressure exceeds the thermal pressure in the underdense coronal plasma. This has two effects: The coronal plasma is expelled from the focal region, and the critical density surface is accelerated into the solid density plasma with a velocity approaching $c/40$, resulting in a steepened density profile very similar to that assumed by Gibbon.

Figure 3(a) shows a plot of energy conversion efficiency in each harmonic vs harmonic order for different irradiances, assuming isotropic emission. It is interesting to note two features. First, the energy in each of the harmonics increases sharply with higher laser irradiance. Second, the energy conversion into each harmonic E_ω for irradiances below 10^{19} W $\mu\text{m}^2\text{cm}^{-2}$ scales as

$$E_\omega = E_{\text{laser}}(\omega/\omega_0)^{-x}, \quad (1)$$

where the exponent x is a function of the irradiance on target. The exponent fitted through all these harmonics decreases with increasing irradiance, changing from $x = 5.5$ at $I\lambda^2 = 5 \times 10^{17}$ W $\mu\text{m}^2\text{cm}^{-2}$ to $x = 3.38$ at $I\lambda^2 = 1.0 \times 10^{19}$ W $\mu\text{m}^2\text{cm}^{-2}$. These values of the exponent are in very good agreement with those predicted by PIC

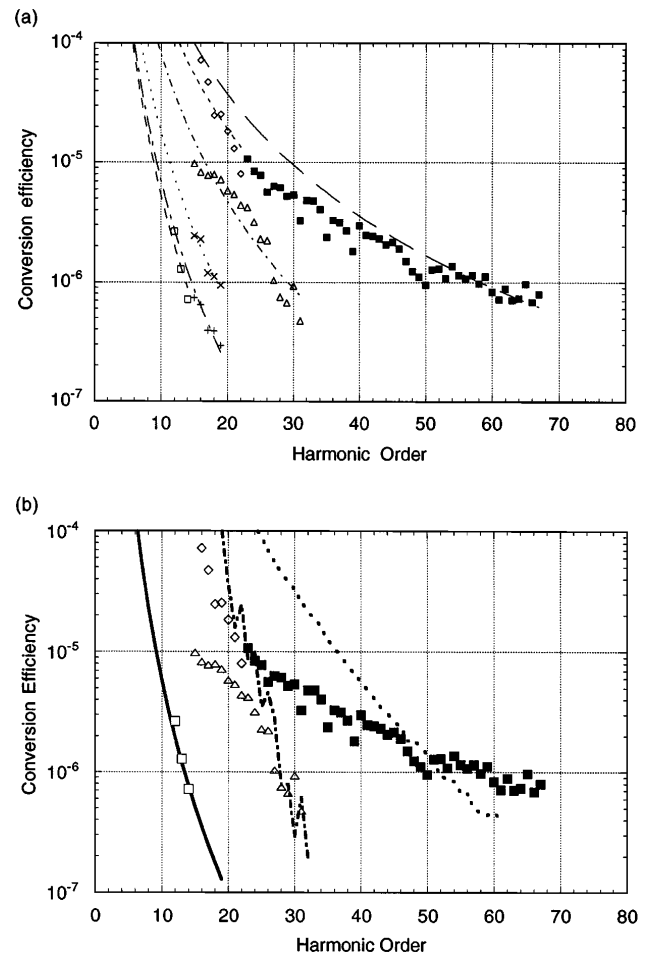


FIG. 3. Conversion efficiencies (assuming isotropic radiation) against harmonic order for various irradiances. Solid squares, $I\lambda^2 = 1.0 \times 10^{19}$ W $\mu\text{m}^2\text{cm}^{-2}$; open diamonds, $I\lambda^2 = 6.3 \times 10^{18}$ W $\mu\text{m}^2\text{cm}^{-2}$; open triangles, $I\lambda^2 = 5.5 \times 10^{18}$ W $\mu\text{m}^2\text{cm}^{-2}$; diagonal crosses, $I\lambda^2 = 3.0 \times 10^{18}$ W $\mu\text{m}^2\text{cm}^{-2}$; horizontal crosses, $I\lambda^2 = 2.5 \times 10^{18}$ W $\mu\text{m}^2\text{cm}^{-2}$; and open squares, $I\lambda^2 = 4.7 \times 10^{17}$ W $\mu\text{m}^2\text{cm}^{-2}$. Curve fits in (a) are best power law fits, except for $I\lambda^2 = 1.0 \times 10^{19}$ W $\mu\text{m}^2\text{cm}^{-2}$ where the curve is fitted to the 50–68th harmonic to illustrate the onset of saturation for the lower harmonics and in (b) are theoretical calculations of the absolute conversion efficiency for 5×10^{17} W $\mu\text{m}^2\text{cm}^{-2}$ (solid line), 5×10^{18} W $\mu\text{m}^2\text{cm}^{-2}$ (chain), and 1.0×10^{19} W $\mu\text{m}^2\text{cm}^{-2}$ (dotted line).

calculations, assuming a density scale length of $L/\lambda = 0.02$ [23] [see Fig. 3(b)]. Figure 3 also suggests that the transfer of energy into lower harmonics is starting to saturate at irradiances of $I\lambda^2 = 1.0 \times 10^{19}$ W $\mu\text{m}^2\text{cm}^{-2}$ because they are systematically lower than the fitted power law for the 50–68th harmonic orders suggests. This saturation behavior as the irradiance is increased is also exhibited by PIC calculations and lends some credence to the choice of the scaling law fit.

It is interesting to note that for the 38th harmonic the power is 1.8 MW sr^{-1} at an irradiance of 1.0×10^{19} W $\mu\text{m}^2\text{cm}^{-2}$. If isotropic emission is assumed,

then the power radiated in this harmonic is 24 MW, and the conversion efficiency of energy into each harmonic up to the 68th is $\geq 10^{-6}$. This is also in good agreement with simulations, taking into account the angular spread of emission observed in the experiment. We have observed that there is no clearly defined cutoff in the harmonic spectra. Instead the harmonics fall into the time integrated background emission. This does not of itself demonstrate that there is no cutoff in the harmonic spectrum (given by the maximum observed harmonic order $n_{\max}^2 = n_u/n_{\text{critical}}$) corresponding to an upper shelf density n_u , as predicted by Carman, Forslund, and Kindel [18]. However, if the Carman, Forslund, and Kindel theory is correct, the upper shelf density corresponding to the highest harmonic observed would be $n_e = 6 \times 10^{24} \text{ cm}^{-3}$. This corresponds to 17 times solid density, which is barely credible. Furthermore, the good agreement in absolute conversion efficiency between our experiment and Gibbon's simulation for irradiances up to 5×10^{18} [shown in Fig. 3(b)] tilts the balance firmly in favor of Gibbon's [23] interpretation (i.e., the cutoff previously reported is an artifact of the low temporal and spatial resolution used in the Carman, Forslund, and Kindel calculation [18]). The discrepancy at the highest irradiance can be accounted for by pulse shape effects starting to become important (the PIC simulation uses a trapezoidal rather than a sech² pulse). It is also worth noting that the 56th harmonic of an ultraviolet laser such as KrF is in the "water window" of the spectrum, and the intensity requirement, inferred from these data and Gibbon's calculations, for obtaining this harmonic is $1.5 \times 10^{20} \text{ W cm}^{-2}$. High brightness KrF lasers that can deliver this intensity are currently under construction [31].

In conclusion, we have observed harmonic orders up to the 68th at 15.5 nm in first-order diffraction and indications of the 75th in second-order diffraction at 14.0 nm. These were created during the interaction of a 2.5 ps, 1053 nm laser pulse with a solid target for irradiances of $1.0 \times 10^{19} \text{ W } \mu\text{m}^2 \text{ cm}^{-2}$. The dependence of both the number of harmonics and their energy conversion efficiency with intensity have been explored. We have shown that there is little difference in the harmonic spectra between both *s* and *p* polarizations of the laser beam and with the addition of a prepulse. The power into the high harmonics is comparable to the output power of saturated collisional XUV lasers at similar wavelengths.

This work was jointly funded by the United Kingdom Engineering and Physical Sciences Research Council and the European Communities Large Facilities Access Programme. The authors gratefully acknowledge the support of laser operations, target preparation, and engineering

support groups of the Central Laser Facility of the Rutherford Appleton Laboratory.

-
- [1] B. W. Shore and P. L. Knight, *J. Phys. B* **20**, 413 (1987).
 - [2] A. McPherson *et al.*, *J. Opt. Soc. Am. B* **4**, 595 (1987).
 - [3] X. F. Li *et al.*, *Phys. Rev. A* **39**, 5751 (1989).
 - [4] A. L'Huillier, K. J. Schafer, and K. C. Kulander, *Phys. Rev. Lett.* **66**, 2200 (1991).
 - [5] N. Sarukura *et al.*, *Phys. Rev. A* **43**, 1669 (1991).
 - [6] J. W. G. Tisch *et al.*, *Phys. Rev. A* **49**, R28 (1994).
 - [7] C.-G. Wahlstrom *et al.*, *Phys. Rev. A* **48**, 4709 (1993).
 - [8] T. Ditmire, J. K. Crane, H. Nguyen, L. B. DaSilva, and M. D. Perry, *Phys. Rev. A* **51**, R902 (1995).
 - [9] S. Watanabe *et al.*, *Phys. Rev. Lett.* **73**, 2692 (1994).
 - [10] M. D. Perry and G. Mourou, *Science* **264**, 917 (1994).
 - [11] J. J. Macklin, J. D. Kmetec, and C. L. Gordon III, *Phys. Rev. Lett.* **70**, 766 (1993).
 - [12] S. G. Preston *et al.*, *Phys. Rev. A* **53**, 31 (1996).
 - [13] S. C. Wilks, W. L. Kruer, and W. B. Mori, *IEEE Trans. Plasma Sci.* **21**, 120 (1993).
 - [14] S. V. Bulanov, N. M. Naumova, and F. Pegoraro, *Phys. Plasmas* **1**, 745 (1994).
 - [15] S. Kohlweyer *et al.*, *Opt. Commun.* **117**, 431 (1995).
 - [16] R. Lichters and J. Meyer-ter-Vehn, *Gesellschaft für Schwerionenforschung, Darmstadt Report No. GSI-95-06, 1995*, p. 64, ISSN 0171-4546.
 - [17] D. von der Linde *et al.*, *Phys. Rev. A* **52**, R25 (1995).
 - [18] R. L. Carman, D. W. Forslund, and J. M. Kindel, *Phys. Rev. Lett.* **46**, 29 (1981).
 - [19] B. Bezzerides, R. D. Jones, and D. W. Forslund, *Phys. Rev. Lett.* **49**, 202 (1982).
 - [20] R. L. Carman, C. K. Rhodes, and R. F. Benjamin, *Phys. Rev. A* **24**, 2649 (1981).
 - [21] N. H. Burnett *et al.*, *Appl. Phys. Lett.* **31**, 172 (1977).
 - [22] C. Grebogi *et al.*, *Phys. Fluids* **26**, 1904 (1983).
 - [23] P. Gibbon, *Phys. Rev. Lett.* **76**, 50 (1996).
 - [24] C. N. Danson *et al.*, *Opt. Commun.* **103**, 392 (1993).
 - [25] A. P. Fews, M. J. Lamb, M. Savage, *Opt. Commun.* **94**, 259 (1992).
 - [26] A. P. Fews *et al.*, *Phys. Rev. Lett.* **73**, 1801 (1994).
 - [27] D. Neely, A. Damerell, R. Parker, and M. Zepf, *Central Laser Facility Annual Report, Rutherford Appleton Laboratory Technical Report No. RAL-TR-95-025, 1995*, pp. 113,114.
 - [28] M. Zepf *et al.*, *Central Laser Facility Annual Report 1995, Rutherford Appleton Laboratory Technical Report No. RAL-TR- 95-025, 1995*, pp. 115,116.
 - [29] S. C. Wilks *et al.*, *Phys. Rev. Lett.* **69**, 1383 (1992).
 - [30] A. Pukhov and J. Meyer-ter-Vehn, *Gesellschaft für schwerionenforschung, Darmstadt Report No. GSI-95-06, 1995*, pp. 42,43, ISSN 0171-4546.
 - [31] Specifications for the TITANIA KrF laser system, S. M. Angood *et al.*, *Rutherford Appleton Laboratory Report No. RAL 94-014, 1994*.